Delayed autumn phenology in the Northern Hemisphere is related to change in both climate and spring phenology

Delayed autumn phenology in the Northern Hemisphere is related to change in both climate and spring phenology

Qiang Liu[1], Yongshuo H. Fu[1,2], Zaichun Zhu[1], Yongwen Liu[1],

Zhuo Liu[1], Mengtian Huang[1], Ivan A. Janssens[2], Shilong Piao[1,3*]

[1] Sino-French Institute for Earth System Science, College of Urban and Environmental Sciences, Peking University, Beijing 100871, China

[2] Centre of Excellence PLECO (Plant and Vegetation Ecology), Department of Biology, University of Antwerp, Universiteitsplein 1, B-2610 Wilrijk, Belgium

[3] Institute of Tibetan Plateau Research, Center for Excellence in Tibetan Earth Science, Chinese Academy of Sciences, Beijing 100085, China.

Running title: Spring phenology affects autumn phenology

Keywords: Autumn phenology, End of growing season, climate change, Spring phenology, NDVI

Manuscript for *Global Change Biology*

**** Corresponding author***

Abstract

The timing of the end of the vegetation growing season (EOS) plays a key role in terrestrial ecosystem carbon and nutrient cycles. Autumn phenology is, however, still poorly understood and previous studies generally focused on few species or were very limited in scale. In this study, we applied four methods to extract EOS dates from NDVI records between 1982 and 2011 for the northern hemisphere, and determined the temporal correlations between EOS and environmental factors (i.e. temperature, precipitation and insolation), as well as the correlation between spring and autumn phenology, using partial correlation analyses. Overall, we observed trend towards later EOS in ~ 70% of the pixels in Northern Hemisphere, with a mean rate of 0.18 ± 0.38 days per year. Warming preseason temperature was positively associated with the rate of EOS in most of our study area, except for arid/semi-arid regions, where the precipitation sum played a dominant positive role. Interestingly, increased preseason insolation sum might also lead to a later date of EOS. In addition to the climatic effects on EOS, we found an influence of spring vegetation green-up dates (SOS) on EOS, albeit biome dependent. Our study, therefore, suggests that both environmental factors and spring phenology should be included in the modeling of EOS to improve the predictions of autumn phenology as well as our understanding of the global carbon and nutrient balances.

Introduction

The timing of phenological events, such as start of the growing season (SOS) and end of the growing season (EOS), is particularly sensitive to climate change (Chuine *et al.*, 2004; Menzel *et al.*, 2006; Stocker *et al.*, 2013; Fu *et al.*, 2015b). Previous studies, however, have mainly focused on SOS (Schwartz *et al.*, 2006; Cleland *et al.*, 2007; Fu *et al.*, 2014b; Guo *et al.*, 2015) and investigations of the response of EOS to climate change are much fewer (Miloud & Ali, 2012; Gallinat *et al.*, 2015). Recent studies, however, reported that EOS dynamics may play a critical role in determining the length of vegetation growing season (Zhu *et al.*, 2012; Garonna *et al.*, 2014), and subsequently regulate terrestrial water, carbon and nutrient cycles (Piao *et al.*, 2008; Richardson *et al.*, 2013; Keenan *et al.*, 2014; Estiarte & Peñuelas, 2015). However, we are still far from understanding the dynamics of autumn vegetation phenology and its associated controls (Klosterman *et al.*, 2014; Estiarte & Peñuelas, 2015). Hence, thorough investigation of EOS and its environmental and physiological controls (i.e. SOS) is needed to promote autumn phenology modeling and increase our understanding of global carbon and nutrient cycles in the context of climate change.

Current knowledge of long-term variation in autumn phenology was generally obtained from ground observations (Menzel *et al.*, 2006; Gill *et al.*, 2015; Panchen *et al.*, 2015). In addition, large spatial and temporal scale analyses facilitated by remote-sensing based phenology data have indicated an overall delayed trend in EOS (Stöckli & Vidale, 2004; Julien & Sobrino, 2009; Garonna *et al.*, 2014). However, large uncertainty occurs within and among these

remote-sensing based EOS estimations, which is mainly associated with the methods that were used to extract EOS dates from the Normalize Differenced Vegetation Index (NDVI) seasonal cycle. These methods of EOS estimation consist of two main procedures. First, elimination of noise from NDVI time-series using smoothing and filtering functions (Roerink *et al.*, 2000; Moody & Johnson, 2001; Chen *et al.*, 2004). Second, determination of EOS based on predefined NDVI thresholds or changing characteristics in temporal profile (Myneni *et al.*, 1997; Zhang *et al.*, 2003; Piao *et al.*, 2006; Julien & Sobrino, 2009; Shen *et al.*, 2014). Given the large differences in EOS estimation among different methods, combining multiple methods are thus preferred when exploring EOS dynamics.

Compared to SOS (Fu *et al.*, 2014b; Ge *et al.*, 2014; Wang *et al.*, 2015), the linkages between EOS and its driving factors are very unclear (Sparks & Menzel, 2002; Menzel *et al.*, 2006). Recent studies reported positive correlations between day length and/or light intensity and EOS dates (Keskitalo *et al.*, 2005; Günter *et al.*, 2008; Borchert *et al.*, 2015; Liu *et al.*, 2015). However, the physiological mechanism of light regulation of EOS is still unclear due to the difficulty in separating the effects of day length (i.e., photoperiod) and light intensity (Calle *et al.*, 2010). In regional investigations of the influence of light fluctuations, solar radiation was used as an integrated measure of both day length and solar intensity (Calle *et al.*, 2010). In the present study, we therefore explored the correlation between EOS and light based on the sum of daily absorbed solar radiation over the time period preceding EOS (referred to as the insolation sum over the preseason). In addition to light effects, recent experimental efforts

have reported that warming during summer and autumn significantly delays the timing of leaf senescence (Gunderson *et al.*, 2012; Marchin *et al.*, 2015), which was consistent with long-term ground observations (Sparks & Menzel, 2002; Ibáñez *et al.*, 2010). Precipitation was also reported to play a role in determining EOS (Richardson *et al.*, 2013; Estiarte & Peñuelas, 2015), especially in arid regions (Liu *et al.*, 2015). Moreover, Fu *et al.* (2014a) reported earlier autumnal senescence as a consequence of warming-induced earlier spring leaf out, using a manipulative warming experiment. However, how these climatic variables and spring phenology determine EOS dates at larger spatial and temporal scales has not been well investigated.

In the present study, we applied four widely used methods to estimate the EOS dates from the long-term satellite NDVI records (1982-2011) from the Global Inventory Modeling and Mapping Studies (GIMMS). The primary objectives of this study are (1) to quantify the change in EOS across the Northern Hemisphere (north of 30°N); (2) to investigate the environmental controls (e.g. temperature, precipitation and insolation) on the date of EOS and (3) to explore the linkage between SOS and EOS.

Materials and Methods

Study area and biomes

Our study was conducted across the Northern Hemisphere, excluding the sub-tropical regions (i.e. latitudes lower than 30 °N) due to their unclear seasonality in vegetation dynamics. Moreover, we excluded pixels dominated with cropland (i.e. referred from MODIS Landover classification product (IGBP) classification, Fig. S1), because their seasonal cycle is largely influenced by human regulation. For the sake of reducing noise resulting from non-vegetation signals, area covered with bare soil/sparse vegetation (i.e. annual mean NDVI lower than 0.1) was also excluded from our analysis (Zhou *et al.*, 2001).

Datasets

Gridded Climate data

In this study, the monthly temperature and precipitation data with a spatial resolution of 0.5x0.5° were extracted from CRU-TS 3.21 climate dataset (Harris *et al.*, 2014) and covered the period from 1982 to 2011. This climate dataset was gridded from archives of meteorological station records across the world's land areas and a previous climatology using a spatial interpolation method (New *et al.*, 2000; Mitchell & Jones, 2005). Monthly insolation data (i.e. the sum of incoming short-wave solar radiation) from 1982-2011 was obtained from the CRU-NCEP datasets with a spatial resolution of 0.5x0.5° (ftp://nacp.ornl.gov/synthesis/2009/frescati/model_driver/cru_ncep/analysis/readme.htm). Both the CRU-TS and CRU-NCEP databases have been applied in recent climate change and

phenological research (Peng *et al.*, 2013; Forkel *et al.*, 2014; Piao *et al.*, 2015).

Satellite NDVI records

NDVI, determined as the ratio of the difference between near-infrared reflectance and red visible reflectance to their sum, is commonly used as a proxy of vegetation greenness and photosynthetic activity (Myneni & Hall, 1995; Myneni *et al.*, 1997). Thus, its seasonal curve could be used to determine the timing of phenological events (e.g. both start and end of growing season) (Buitenwerf *et al.*, 2015; Forkel *et al.*, 2015). In this study, we employed the latest and longest release of satellite NDVI records (referred as $NDVI_{3g}$) by NASA's GIMMS group (Tucker *et al.*, 2004; Tucker *et al.*, 2005). Multiple corrections have been applied to eliminate errors and noise related to change of satellite sensors, atmospheric interference and non-vegetation dynamics (Vermote *et al.*, 1997; Pinzon *et al.*, 2005; Sobrino *et al.*, 2008; Pinzon & Tucker, 2014). It contains fortnightly NDVI observations at a spatial resolution of one-twelfth of a degree (~ 8 km) during the past three decades. We therefore extracted the NDVI pixels with a complete cycle (Jan.1982 - Dec.2011) and assigned the middle of the whole compositing period to the acquisition date of each NDVI image to construct NDVI time-series.

Phenology extraction methods

Numerous methods have been developed to extract SOS and EOS from the seasonal cycle of NDVI. However, NDVI data might be misrepresented by snow (Grippa *et al.*, 2005). In

addition, the performance of phenology extraction methods was reported to be sensitive to the influence of snow coverage during the non-growing season (Shen *et al.*, 2013). Due to the absence of available snow information in the GIMMS $NDVI_{3g}$ dataset, we used daily air temperature (interpolated from monthly temperature data using spline function) and certain criteria (i.e. below 0 °C for a sequence of five days) to screen out pixels that were potentially covered by snow, and subsequently replaced the NDVI estimate with that of the temporally nearest snow-free date. Another purpose of applying this temperature threshold was to ensure that the estimated EOS would not be positioned beyond the thermal growing season. Finally, a five-point median moving average filter was introduced to delete abnormally high/low values in the NDVI cycle, which were subsequently replaced with smoothed value. After this preprocessing of the NDVI data, four methods were applied. The detailed information, including the data filtering function and corresponding criteria used to help determining the date of EOS from the smoothed NDVI seasonal curve, is displayed in Table 1 and supplementary materials. The coefficients of each data filter function were optimized using the Levenberg–Marquardt (LM) method (Moré, 1978), thus changed the biweekly sampled NDVI data resolution on a daily basis. We then applied the relevant criteria to estimate EOS.

Analyses

Linear least squares regression was used to estimate the temporal trends of EOS from 1982 to 2011 at pixel level. Trend analysis was applied in both the ensembles and the individual methods of the four methods to provide robust estimates of the change in EOS across the

Northern Hemisphere. The EOS data and the vegetation map were remapped into the same resolution of the climatic variables (i.e. 0.5x0.5°). Spearman's rank correlation coefficients were used to determine the preseason length that was defined as the period when the highest correlation coefficients occurred between the date of EOS and each of the climatic factors (i.e. temperature mean, precipitation sum and insolation sum) calculated from periods ahead of EOS with a one-month step. The maximum range of this period was set from June to the multi-year average date of EOS following previous studies (Jeong *et al.*, 2011; Yue *et al.*, 2015). The preseason for each of the three climatic factors i.e. temperature mean, precipitation sum and insolation sum, were determined separately. Then, we applied a temporal partial correlation analysis between EOS and mean temperature, precipitation sum, and insolation sum over the preseason, as well as the date of SOS. This technique has been applied in previous studies involving climate change and vegetation phenology (Peng *et al.*, 2013; Fu *et al.*, 2015a; Fu *et al.*, 2015b). The ensemble mean of the partial correlation coefficients were calculated for each and across all biomes.

Results

Changes in autumn phenology and climate in the Northern Hemisphere

During the period 1982 - 2011, the mean date of EOS in the Northern Hemisphere was delayed with an average rate of 0.18 ± 0.38 days per year. More than 70% of the study area experienced delayed trends of EOS, with roughly 43% of them statistically significant at $P < 0.05$ (Fig. 1a, dotted regions). Advanced EOS was, however, mainly observed in arid/semi-arid regions (e.g. Central Asia), Siberia, Northern Eurasia and northwestern North America. Consistent results were found across each of the four individual methods (Fig. S3a, e, i and m).

The optimal length of the preseason ranged between 0 (current month of EOS) and 4 months (i.e. autumn/summer) (Fig. S2), but averaged at 1.4 (temperature), 1.2 (precipitation) and 1.1 (insolation) months preceding the date of EOS (Fig. S2a-c). During the past three decades, increasing temperature was observed in most of the study area (94%), with statistically significant trends (52% of area) occurring mainly in southwestern North America, Northern Canada, Eastern Eurasia and Northern Europe (Fig. 1b). Changes in precipitation and insolation were non-uniform (Fig. 1). Neither positive nor negative trends dominated (both nearly 50%) over the study areas. Nonetheless, decreasing precipitation was detected in Southwestern North America, Central Eurasia and Northern China, and increasing precipitation in Northeastern Canada and Russia. Insolation decreased in Siberia, Northeastern and Western North America, but increased in part of Central North America,

194 Central Eurasia and Northern China. This spatial pattern of changes in climate factors was
195 found in each of the four applied methods (Fig. S3).
196
197 ***Climatic controls on autumn phenology in the Northern Hemisphere***
198 After removing the influence of precipitation, insolation and SOS with the partial correlation
199 approach, we found large positive correlations between temperature and EOS in more than 71%
200 of the study area (around 27% of them were statistically significant at P <0.05). Significant
201 positive correlations were mainly found in Northeastern North America, Northern Europe and
202 Eastern Russia. No statistically significant correlations between preseason temperature and
203 EOS were found in arid/semi-arid Central Asia, suggesting that preseason temperate might
204 not be the primary factor for EOS in dry climate areas (Fig. 2a). For precipitation, we found
205 that neither the positive nor the negative partial correlations dominated the whole regions (Fig.
206 2b). While, negative correlations were observed at high latitudes, such as Northern Europe,
207 Western Canada, Alaska and Western US. In dry regions, e.g. Central North America, Central
208 Eurasia and Northern China, positive correlations were dominated, suggesting that more
209 precipitation in summer/autumn would contribute to a later end of the growing season. The
210 partial correlations between EOS and insolation sum was also spatially different. We found
211 positive correlations mainly at high latitudes, i.e. Siberia, Eastern Russia and Alaska, in more
212 than 65% of the study area. Negative correlations between EOS and insolation were mainly
213 found in temperate regions, but the occurrence was fragmented (Fig. 2c). Our results inferred
214 from the partial correlations were confirmed by simple correlation analysis in both percentage

of positive/negative correlations and their spatial patterns (Fig. 2d-f). In addition, the influence of temperature, precipitation and insolation on EOS was consistently found in each of the four individual methods (Fig. S4-7).

To provide a comprehensive interpretation of the climatic effects on EOS, we show a map of the partial correlation coefficients of the climatic variables with EOS in Northern Hemisphere (Fig. 3a), as well as the distribution of the partial correlation coefficients in climate space (Fig. 3b-d). Consistent with the above results, we found that precipitation associates best with EOS in semi-arid/arid regions, while the temperature plays a key role in cold regions. In detail, we found that precipitation exerts a dominant control over EOS in regions with MAP less than 500 mm and MAT greater than 0 °C. In humid areas (e.g. MAP > 750 mm), the role of temperature is dominant, while in semi-humid (e.g. 350 mm < MAP < 750 mm) and cold regions (e.g. MAT < -5 °C), both temperature and insolation determine the EOS dates. Similar results in term of dominant climatic drivers were found in each of the four methods (Fig. S8a-n).

The influence of spring phenology on autumn phenology in Northern Hemisphere

The correlation between SOS and EOS was investigated using both partial correlation removing impact of temperature, precipitation and insolation (Fig. 4a) and simple correlation (Fig. 4b). Positive correlations were mainly observed in Northern Eurasia, Siberia and Northern North America, while negative correlations occurred in middle latitudes (e.g. eastern

Northern America). Over all, positive correlations dominated and were found in 60% (20% were significant) of our study area for both correlation analyses. Similar results were found for both the partial and simple correlation analysis, and across the individual methods, although in the Piecewise logistic method (Fig. S9g-h), the percentage of positive correlation was relatively lower.

Drivers of autumn phenology at biome level

The biome-dependent partial correlation coefficients between EOS, climatic factors and spring phenology (i.e. SOS) are displayed in Fig. 5. The climatic controls on the date of EOS were substantially different among biomes. Generally, the role of temperature in postponing the date of EOS was clearly observed in forest biomes (more than 85% of pixels of these biomes expressed positive correlations, except for DNF). The influence of precipitation was more dominant in Grasslands (positive in about 73%), while the influence of insolation was evident in forests. SOS played a more critical role in deciduous forests when compared with environmental factors. In detail, the date of EOS of ENF was mainly associated with environmental factors, i.e. temperature (positive correlation at 85% of the area), precipitation (74%) and insolation (70%), and the influence of SOS was ambiguous. For DNF, insolation and SOS were found to be positively associated with EOS at more than 73% and 85% of total pixels, and more approximately one-fifth of them were significant. For DBF, both environmental factor and SOS affected the EOS dates, with a dominance of temperature (95% of DBF area) and SOS (78%). In addition, temperature and precipitation (67%) were

positively associated with EOS, while insolation (61%) and SOS were negatively associated with EOS. The EOS of MF was positively correlated to temperature (86%) and insolation (69%), but negatively correlated to precipitation (69%) and SOS (61%). Compared to forests, the EOS of both shrublands and savannas was generally associated with temperature, insolation and SOS. For Grasslands in contrast, precipitation was the most relevant environmental driver of EOS, dominating in 73% of total pixels (significant in 32%). Furthermore, the influence of SOS (70%) was also stronger compared to temperature (63%) and insolation (52%). The effects of climatic factors and SOS were consistently present in three methods, i.e. Hants-Mr, Polyfit-Mr and Double logistic, while for the Piecewise logistic method, the distribution of positive/negative correlations was slightly different in few biomes (Fig. S10).

Discussion

Changes in EOS in Northern Hemisphere

Using long-term (from 1982 to 2011) satellite NDVI records and four widely used methods to extract EOS, our results revealed a trend of delayed EOS at an average rate of 0.18 ± 0.38 days per year across the Northern Hemisphere. This finding is consistent with previous studies that documented a delay in EOS at regional scale, e.g. Northern America (Reed, 2006; Zhang *et al.*, 2007; Dragoni & Rahman, 2012), Eurasia (Stöckli & Vidale, 2004) and China (Liu *et al.*, 2015). Nonetheless, the differences in the rate of changes in EOS exist among regions and studies, i.e. from 0.19 to 0.45 days per year, which may be related to differences in both methodology and study periods and areas.

We found that a warming climate in summer/autumn delayed the date of EOS in most of the Northern Hemisphere, especially at cold regions (e.g. higher latitudes), which is consistent with previous studies based on field experiments and satellite data (Estrella & Menzel, 2006; Delpierre *et al.*, 2009; Ge *et al.*, 2014; Vitasse *et al.*, 2014). The positive effect of temperature on EOS is likely related to the warming-induced enhancement of activities of photosynthetic enzymes (Shi *et al.*, 2014), to the reduced speed of chlorophyll degradation (Fracheboud *et al.*, 2009), to the reduced probability of being exposed to frost in autumn (Schwartz, 2003; Hartmann *et al.*, 2013), or to the increased potential for growth and photosynthetic consumption. In contrast, we also found negative correlations between temperature and EOS in arid and semi-arid regions, such as in grassland in Central Eurasia. This may be related to

289 the fact that a warmer autumn might critically reduce water availability in dry regions (Dai *et*
290 *al.*, 2004), with negative impacts on plant growth and photosynthesis activity (Tezara *et al.*,
291 1999) and increased risk of chlorophyll degradation and plant mortality (Anderegg *et al.*,
292 2013; Dreesen *et al.*, 2014), and subsequently resulting in earlier EOS. This was further
293 confirmed by the larger positive partial correlation between precipitation and EOS over these
294 regions. We found a negative effect of precipitation on EOS in colder regions (e.g. MAT ≤
295 5°C, Fig. 2, Fig. S4-7, Fig. S11), which may be because high soil moisture can limit nutrient
296 availability for growth in these often permafrost-affected regions (Bonan & Shugart, 1989).
297 Interestingly, we found a positive correlation between insolation and EOS at high latitudes.
298 Increase in insolation have been demonstrated to retard the accumulation of abscisic acid and
299 subsequently slow the speed of leaf senescence (Thimann & Satler, 1979a; Thimann & Satler,
300 1979b; Gepstein & Thimann, 1980). Enhanced photosynthetic capacity, CO_2 sequestration
301 rate (Bonan, 2002) and chlorophyll levels (He *et al.*, 2005; Kim *et al.*, 2008) also contributed
302 to the delaying effect of greater insolation on EOS. Thus, the delayed trends at high latitudes
303 induced by rising temperature could also be dampened by a decrease in availability of
304 insolation, especially in Siberia.
305
306 At biome level, the positive influence of temperature was more pronounced in forest than in
307 grasslands. EOS of DNF was primarily regulated by insolation and SOS, while for DBF, all
308 factors were associated with the date of EOS. For grassland, although precipitation dominated
309 the change in EOS, temperature and SOS should also be considered. Overall, there is still no

consensus on which factors could eventually determine the process of autumn phenology, the correlation between EOS and climatic factors was complex and more manipulative experiments focusing on EOS phenology, are clearly needed to explore the mechanisms behind the observed delayed trend of autumn phenology.

The influence of spring phenology on autumn phenology

Besides the climatic controls on EOS, we also observed additional effects of spring phenology on autumn phenology in line with a recent experimental study (Fu *et al.*, 2014a) and remote sensing-based studies (Keenan & Richardson, 2015; Wu *et al.*, 2016). Multiple mechanisms have been proposed to explain the carryover effects of SOS (i.e. earlier SOS is followed by an earlier date of EOS). 1) The timing of leaf senescence was reported to be constrained by factors associated with leaf traits directly, such as leaf life span (Reich *et al.*, 1992) and programmed cell death (Lim *et al.*, 2007). 2) Earlier spring might lead to soil water loss in the early part of growing season, thereby increasing the prevalence of drought during summer (Buermann *et al.*, 2013) that may subsequently result in earlier leaf senescence. 3) Earlier leaf emergence may increase the risk of being exposed to spring frost (Hufkens *et al.*, 2012), and the outbreak of harmful insects (Jepsen *et al.*, 2011), which may be related to earlier leaf senescence. 4) The correlation between SOS and EOS was also suggested to be related to the limitation in the size of the plants' carbon sink: earlier accumulation of non-structural carbohydrate in spring might have contributed to the earlier achievement of its maximum carbon content in autumn (Charrier & Améglio, 2011; Fu *et al.*, 2014a). Nonetheless, it should

be noted that the influence of earlier SOS on the determination of EOS was weaker than climatic variables across all biomes, and even in some areas with deciduous forest, a negative correlation were founded, suggesting more experimental efforts are needed to improve the understanding of the climatic and SOS effects on the EOS phenology process.

In conclusion, using four widely accepted EOS extraction methods and satellite derived NDVI records from 1982 to 2011, we found an overall trend of delayed EOS across the Northern Hemisphere. Our study revealed the different dominant drivers of EOS dynamics at spatial and biome level. Warming temperature postponed the date of EOS in most (~ 70%) of our study area, except for arid/semi-arid regions (e.g. Central Eurasia). Increased precipitation at high latitudes lead to earlier EOS, while sufficient insolation would facilitate the prolongation of the growing season in autumn. Moreover, we confirmed additional influence of SOS on EOS, which displayed positive correlations in high latitudes and negative correlations mainly in eastern North America. Multiple factors regulate the date of EOS at biome level. Except for temperature, effects of precipitation were also clearly observed, especially in ENF and grassland. The influence of insolation was mainly evident in forests. SOS played a significant role in DNF and DBF when compared with climate factors. Our study, therefore, suggests that both climatic factors and SOS should be considered in the modeling and simulation of EOS and to improve our understanding of EOS phenology responses to future climate change scenarios.

Acknowledgements

This study was supported by the National Natural Science Foundation of China (41561134016 and 41530528), and National Youth Top-notch Talent Support Program in China.

References:

Anderegg WR, Plavcová L, Anderegg LD, Hacke UG, Berry JA, Field CB (2013) Drought's legacy: multiyear hydraulic deterioration underlies widespread aspen forest die-off and portends increased future risk. Global Change Biology, **19**, 1188-1196.

Bonan GB, Shugart HH (1989) Environmental factors and ecological processes in boreal forests. Annual review of ecology and systematics,**20**, 1-28.

Borchert R, Calle Z, Strahler AH *et al.* (2015) Insolation and photoperiodic control of tree development near the equator. New Phytologist, **205**, 7-13.

Buermann W, Bikash PR, Jung M, Burn DH, Reichstein M (2013) Earlier springs decrease peak summer productivity in North American boreal forests. Environmental Research Letters, **8**, 024027, doi:10.1088/1748-9326/8/2/024027.

Buitenwerf R, Rose L, Higgins SI (2015) Three decades of multi-dimensional change in global leaf phenology. Nature Climate Change, **5**, 364–368.

Calle Z, Schlumpberger BO, Piedrahita L, Leftin A, Hammer SA, Tye A, Borchert R (2010) Seasonal variation in daily insolation induces synchronous bud break and flowering in the tropics. Trees, **24**, 865-877.

Charrier G, Améglio T (2011) The timing of leaf fall affects cold acclimation by interactions

with air temperature through water and carbohydrate contents. Environmental and Experimental Botany, **72**, 351-357.

Chen J, Jönsson P, Tamura M, Gu Z, Matsushita B, Eklundh L (2004) A simple method for reconstructing a high-quality NDVI time-series data set based on the Savitzky–Golay filter. Remote Sensing of Environment, **91**, 332-344.

Chuine I, Yiou P, Viovy N, Seguin B, Daux V, Ladurie ELR (2004) Historical phenology: grape ripening as a past climate indicator. Nature, **432**, 289-290.

Cleland EE, Chuine I, Menzel A, Mooney HA, Schwartz MD (2007) Shifting plant phenology in response to global change. Trends in ecology & evolution, **22**, 357-365.

Dai A, Trenberth KE, Qian T (2004) A global dataset of Palmer Drought Severity Index for 1870-2002: Relationship with soil moisture and effects of surface warming. Journal of Hydrometeorology, **5**, 1117-1130.

De WitA, Su B (2005) Deriving phenological indicators from SPOT-VGT data using the HANTS algorithm. In: 2nd International SPOT-VEGETATION User Conference, pp. 195–201. Centre National d'Etudes Spatiales, Antwerp, Belgium.

Delpierre N, Dufrêne E, Soudani K, Ulrich E, Cecchini S, Boé J, François C (2009) Modelling interannual and spatial variability of leaf senescence for three deciduous tree species in France. Agricultural and Forest Meteorology, **149**, 938-948.

Dragoni D, Rahman AF (2012) Trends in fall phenology across the deciduous forests of the Eastern USA. Agricultural and Forest Meteorology, **157**, 96-105.

Dreesen F, De Boeck H, Janssens I, Nijs I (2014) Do successive climate extremes weaken the

394 resistance of plant communities? An experimental study using plant assemblages.
395 Biogeosciences, **11**, 109-121.
396 Estiarte M, Peñuelas J (2015) Alteration of the phenology of leaf senescence and fall in winter
397 deciduous species by climate change: effects on nutrient proficiency. Global Change
398 Biology, **21**, 1005–1017.
399 Estrella N, Menzel A (2006) Responses of leaf colouring in four deciduous tree species to
400 climate and weather in Germany. Climate Research, **32**, 253-267.
401 Forkel M, Carvalhais N, Schaphoff S, Migliavacca M, Thurner M, Thonicke K (2014)
402 Identifying environmental controls on vegetation greenness phenology through
403 model–data integration. Biogeosciences, **11**, 7025-7050.
404 Forkel M, Migliavacca M, Thonicke K, Reichstein M, Schaphoff S, Weber U, Carvalhais N
405 (2015) Co-dominant water control on global inter-annual variability and trends in land
406 surface phenology and greenness. Global Change Biology, **21**: 3414–3435.
407 Fracheboud Y, Luquez V, Björkén L, Sjödin A, Tuominen H, Jansson S (2009) The control of
408 autumn senescence in European aspen. Plant Physiology, **149**, 1982-1991.
409 Fu YH, Campioli M, Vitasse Y *et al.* (2014a) Variation in leaf flushing date influences
410 autumnal senescence and next year's flushing date in two temperate tree species.
411 Proceedings of the National Academy of Sciences, **111**, 7355-7360.
412 Fu YH, Piao S, Op De Beeck M *et al.* (2014b) Recent spring phenology shifts in western
413 Central Europe based on multiscale observations. Global Ecology and Biogeography,
414 **23**, 1255-1263.

Fu YH, Piao S, Vitasse Y *et al.* (2015a) Increased heat requirement for leaf flushing in temperate woody species over 1980-2012: effects of chilling, precipitation and insolation. Global Change Biology, **21**: 2687–2697.

Fu YH, Zhao H, Piao S *et al.* (2015b) Declining global warming effects on the phenology of spring leaf unfolding. Nature, **526**,104–107.

Günter S, Stimm B, Cabrera M *et al.* (2008) Tree phenology in montane forests of southern Ecuador can be explained by precipitation, radiation and photoperiodic control. Journal of Tropical Ecology, **24**, 247-258.

Gallinat AS, Primack RB, Wagner DL (2015) Autumn, the neglected season in climate change research. Trends in ecology & evolution, **30**, 169-176.

Garonna I, De Jong R, De Wit AJW, Mücher CA, Schmid B, Schaepman M (2014) Strong contribution of autumn phenology to changes in satellite-derived growing season length estimates across Europe (1982–2011). Global Change Biology, **20**, 3457-3470.

Ge Q, Wang H, Dai J (2014) Phenological response to climate change in China: a meta-analysis. Global Change Biology, **21**, 265-274.

Gepstein S, Thimann KV (1980) Changes in the abscisic acid content of oat leaves during senescence. Proceedings of the National Academy of Sciences, **77**, 2050-2053.

Gill AL, Gallinat AS, Sanders-Demott R, Rigden AJ, Gianotti DJS, Mantooth JA, Templer PH (2015) Changes in autumn senescence in northern hemisphere deciduous trees: a meta-analysis of autumn phenology studies. Annals of Botany, doi:10.1093/aob/mcv055,.

436 Grippa M, Kergoat L, Le Toan T, Mognard N, Delbart N, L'hermitte J, Vicente-Serrano S
437 (2005) The impact of snow depth and snowmelt on the vegetation variability over
438 central Siberia. Geophysical Research Letters, **32**, L21412,
439 doi:10.1029/2005GL024286.
440 Gunderson CA, Edwards NT, Walker AV, O'hara KH, Campion CM, Hanson PJ (2012) Forest
441 phenology and a warmer climate–growing season extension in relation to climatic
442 provenance. Global Change Biology, **18**, 2008-2025.
443 Guo L, Dai J, Wang M, Xu J, Luedeling E (2015) Responses of spring phenology in temperate
444 zone trees to climate warming: A case study of apricot flowering in China.
445 Agricultural and Forest Meteorology, **201**, 1-7.
446 Harris I, Jones P, Osborn T, Lister D (2014) Updated high-resolution grids of monthly
447 climatic observations–the CRU TS3. 10 Dataset. International Journal of Climatology,
448 **34**, 623-642.
449 Hartmann D, Klein Tank A, Rusicucci M *et al.* (2013) Observations: atmosphere and surface.
450 In: *Climate Change 2013: The Physical Science Basis. Contribution of Working Group*
451 *I to the Fifth Assessment Report of the Intergovernmental Panel on Climate Change.*
452 pp 159-254. Cambridge University Press, Cambridge, United Kingdom and New York,
453 NY, USA.
454 He P, Osaki M, Takebe M, Shinano T, Wasaki J (2005) Endogenous hormones and expression
455 of senescence-related genes in different senescent types of maize. Journal of
456 experimental botany, **56**, 1117-1128.

Hufkens K, Friedl MA, Keenan TF, Sonnentag O, Bailey A, O'keefe J, Richardson AD (2012) Ecological impacts of a widespread frost event following early spring leaf-out. Global Change Biology, **18**, 2365-2377.

Ibáñez I, Primack RB, Miller-Rushing AJ *et al.* (2010) Forecasting phenology under global warming. Philosophical Transactions of the Royal Society of London B: Biological Sciences, **365**, 3247-3260.

Jakubauskas ME, Legates DR, Kastens JH (2001) Harmonic analysis of time-series AVHRR NDVI data. Photogrammetric Engineering and Remote Sensing, **67**, 461-470.

Jeong SJ, Ho CH, Gim HJ, Brown ME (2011) Phenology shifts at start vs. end of growing season in temperate vegetation over the Northern Hemisphere for the period 1982–2008. Global Change Biology, **17**, 2385-2399.

Jepsen JU, Kapari L, Hagen SB, Schott T, Vindstad OPL, Nilssen AC, Ims RA (2011) Rapid northwards expansion of a forest insect pest attributed to spring phenology matching with sub-Arctic birch. Global Change Biology, **17**, 2071-2083.

Julien Y, Sobrino J (2009) Global land surface phenology trends from GIMMS database. International Journal of Remote Sensing, **30**, 3495-3513.

Keenan TF, Gray J, Friedl MA *et al.* (2014) Net carbon uptake has increased through warming-induced changes in temperate forest phenology. Nature Climate Change, **4**, 598-604.

Keenan TF, Richardson AD (2015) The timing of autumn senescence is affected by the time of spring phenology: implications for predictive models. Global Change Biology, **21**:

2634-2641.

Keskitalo J, Bergquist G, Gardeström P, Jansson S (2005) A cellular timetable of autumn senescence. Plant Physiology, **139**, 1635-1648.

Kim J-H, Moon YR, Wi SG, Kim J-S, Lee MH, Chung BY (2008) Differential radiation sensitivities of Arabidopsis plants at various developmental stages. In: Photosynthesis. Energy from the Sun, pp. 1491-1495. Springer, the Netherlands.

Klosterman S, Hufkens K, Gray J *et al.* (2014) Evaluating remote sensing of deciduous forest phenology at multiple spatial scales using PhenoCam imagery, Biogeosciences Discuss, **11**, 2305-2342.

Lim PO, Kim HJ, Gil Nam H (2007) Leaf senescence. Annual Review of Plant Physiology, **58**, 115-136.

Liu Q, Fu YH, Zeng Z, Huang M, Li X, Piao S (2015) Temperature, precipitation, and insolation effects on autumn vegetation phenology in temperate China. Global Change Biology. doi:10.1111/gcb.13081.

Marchin RM, Salk CF, Hoffmann WA, Dunn RR (2015) Temperature alone does not explain phenological variation of diverse temperate plants under experimental warming. Global Change Biology, **21**, 3138-3151.

Menzel A, Sparks TH, Estrella N *et al.* (2006) European phenological response to climate change matches the warming pattern. Global Change Biology, **12**, 1969-1976.

Miloud H, Ali G (2012) *Some aspects of leaf senescence*, INTECH Open Access Publisher, Rijeka.

499 Mitchell TD, Jones PD (2005) An improved method of constructing a database of monthly
500 climate observations and associated high-resolution grids. International Journal of
501 Climatology, **25**, 693-712.
502 Moody A, Johnson DM (2001) Land-surface phenologies from AVHRR using the discrete
503 Fourier transform. Remote Sensing of Environment, **75**, 305-323.
504 Moré JJ (1978) The Levenberg-Marquardt algorithm: implementation and theory. In:
505 *Numerical analysis.* pp. 105-116. Springer, Berlin.
506 Myneni RB, Hall FG (1995) The interpretation of spectral vegetation indexes. Geoscience and
507 Remote Sensing, IEEE Transactions on, **33**, 481-486.
508 Myneni RB, Keeling C, Tucker C, Asrar G, Nemani R (1997) Increased plant growth in the
509 northern high latitudes from 1981 to 1991. Nature, **386**, 698-702.
510 New M, Hulme M, Jones P (2000) Representing twentieth-century space-time climate
511 variability. Part II: Development of 1901-96 monthly grids of terrestrial surface
512 climate. Journal of Climate, **13**, 2217-2238.
513 Panchen ZA, Primack RB, Gallinat AS, Nordt B, Stevens AD, Du Y, Fahey R (2015)
514 Substantial variation in leaf senescence times among 1360 temperate woody plant
515 species: implications for phenology and ecosystem processes. Annals of Botany, doi:
516 10.1093/aob/mcv015.
517 Peng S, Piao S, Ciais P *et al.* (2013) Asymmetric effects of daytime and night-time warming
518 on Northern Hemisphere vegetation. Nature, **501**, 88-92.
519 Piao S, Ciais P, Friedlingstein P *et al.* (2008) Net carbon dioxide losses of northern

ecosystems in response to autumn warming. Nature, **451**, 49-52.

Piao S Fang J, Zhou L, Ciais P, Zhu B (2006) Variations in satellite-derived phenology in China's temperate vegetation. Global Change Biology, **12**, 672-685.

Piao S, Tan J, Chen A *et al.* (2015) Leaf onset in the northern hemisphere triggered by daytime temperature. Nature Communications, **6**, doi:10.1038/ncomms7911.

Pinty B, T. Lavergne, M. Voßbeck, T. Kaminski O *et al.* (2007) Retrieving surface parameters for climate models from Moderate Resolution Imaging Spectroradiometer (MODIS)-Multiangle Imaging Spectroradiometer (MISR) albedo products Journal of Geophysical Research, **112**, D10116, doi:10.1029/2006JD008105.

Pinzon JE, Brown ME, Tucker CJ (2005) Satellite time series correction of orbital drift artifacts using empirical mode decomposition. In: Hilbert-Huang Transform: Introduction and Applications. (ed. Huang N), pp. 167-186. World Scientific Publishing Co. Pte. Ltd, Singapore.

Pinzon JE, Tucker CJ (2014) A non-stationary 1981–2012 AVHRR NDVI3g time series. Remote Sensing, **6**, 6929-6960.

Reed C (2006) Trend analysis of time-series phenology of North America derived from satellite data. GIScience & Remote Sensing, **43**, 24-38.

Reich P, Walters M, Ellsworth D (1992) Leaf life-span in relation to leaf, plant, and stand characteristics among diverse ecosystems. Ecological monographs, **62**, 365-392.

Richardson AD, Keenan TF, Migliavacca M, Ryu Y, Sonnentag O, Toomey M (2013) Climate change, phenology, and phenological control of vegetation feedbacks to the climate

system. Agricultural and Forest Meteorology, **169**, 156-173.

Roerink G, Menenti M, Verhoef W (2000) Reconstructing cloudfree NDVI composites using Fourier analysis of time series. International Journal of Remote Sensing, **21**, 1911-1917.

Schwartz MD (2003) *Phenology: an integrative environmental science*, Springer, Dordrecht.

Schwartz MD, Ahas R, Aasa A (2006) Onset of spring starting earlier across the Northern Hemisphere. Global Change Biology, **12**, 343-351.

Shen M, Sun Z, Wang S, Zhang G, Kong W, Chen A, Piao S (2013) No evidence of continuously advanced green-up dates in the Tibetan Plateau over the last decade. Proceedings of the National Academy of Sciences, **110**, E2329-E2329.

Shen M, Zhang G, Cong N, Wang S, Kong W, Piao S (2014) Increasing altitudinal gradient of spring vegetation phenology during the last decade on the Qinghai–Tibetan Plateau. Agricultural and Forest Meteorology, **189-190**, 71-80.

Shi C, Sun G, Zhang H, Xiao B, Ze B, Zhang N, Wu N (2014) Effects of warming on chlorophyll degradation and carbohydrate accumulation of Alpine herbaceous species during plant senescence on the Tibetan Plateau. Plos one, **9**, e107874, doi: 10.1371/journal.pone.0107874.

Sobrino JA, Julien Y, Atitar M, Nerry F (2008) NOAA-AVHRR orbital drift correction from solar zenithal angle data. Geoscience and Remote Sensing, IEEE Transactions on, **46**, 4014-4019.

Sparks TH, Menzel A (2002) Observed changes in seasons: an overview. International Journal

of Climatology, **22**, 1715-1725.

Stöckli R, Vidale PL (2004) European plant phenology and climate as seen in a 20-year AVHRR land-surface parameter dataset. International Journal of Remote Sensing, **25**, 3303-3330.

Stocker T, Qin D, Plattner G *et al.* (2013) IPCC, 2013: Summary for Policymakers. In Climate Change 2013: The Physical Science Basis. Contribution of Working Group I to the Fifth Assessment Report of the Intergovernmental Panel on Climate Change, Cambridge Univ. Press, Cambridge, UK.

Tezara W, Mitchell V, Driscoll S, Lawlor D (1999) Water stress inhibits plant photosynthesis by decreasing coupling factor and ATP. Nature, **401**, 914-917.

Thimann KV, Satler S (1979a) Relation between leaf senescence and stomatal closure: Senescence in light. Proceedings of the National Academy of Sciences, **76**, 2295-2298.

Thimann KV, Satler S (1979b) Relation between senescence and stomatal opening: Senescence in darkness. Proceedings of the National Academy of Sciences, **76**, 2770-2773.

Tucker CJ, Pinzon JE, Brown ME (2004) Global Inventory Modeling and Mapping Studies, NA94apr15b. n11--VIg, 2. 0, Global Land Cover Facility, University of Maryland, College Park, Maryland.

Tucker CJ, Pinzon JE, Brown ME *et al.* (2005) An extended AVHRR 8-km NDVI dataset compatible with MODIS and SPOT vegetation NDVI data. International Journal of

583 Remote Sensing, **26**, 4485-4498.

584 Vermote E, Saleous NE, Kaufman Y, Dutton E (1997) Data pre-processing: Stratospheric
585 aerosol perturbing effect on the remote sensing of vegetation: Correction method for
586 the composite NDVI after the Pinatubo eruption. Remote Sensing Reviews, **15**, 7-21.

587 VitasseY, Lenz A, Korner C (2014) The interaction between freezing tolerance and phenology
588 in temperate deciduous trees. Frontiers in Plant Science, **5**, 541, doi:
589 10.3389/fpls.2014.00541.

590 Wang X, Piao S, Xu X, Ciais P, Macbean N, Myneni RB, Li L (2015) Has the advancing onset
591 of spring vegetation green-up slowed down or changed abruptly over the last three
592 decades? Global Ecology and Biogeography, **24**, 621-631..

593 Wu C, Hou X, Peng D, Gonsamo A, Xu S (2016) Land surface phenology of China's
594 temperate ecosystems over 1999–2013: Spatial–temporal patterns, interaction effects,
595 covariation with climate and implications for productivity. Agricultural and Forest
596 Meteorology, **216**, 177-187.

597 Yue X, Unger N, Keenan TF, Zhang X, Vogel CS (2015) Probing the past 30 year phenology
598 trend of US deciduous forests. Biogeosciences Discussions, **12**, 6037-6080.

599 Zhang X, Friedl MA, Schaaf CB *et al.* (2003) Monitoring vegetation phenology using
600 MODIS. Remote Sensing of Environment, **84**, 471-475.

601 Zhang X, Tarpley D, Sullivan JT (2007) Diverse responses of vegetation phenology to a
602 warming climate. Geophysical Research Letters, **34**, doi:10.1029/2007GL031447.

603 Zhou L, Tucker CJ, Kaufmann RK, Slayback D, Shabanov NV, Myneni RB (2001) Variations

in northern vegetation activity inferred from satellite data of vegetation index during 1981 to 1999. Journal of Geophysical Research: Atmospheres (1984–2012), **106**, 20069-20083.

Zhu W, Tian H, Xu X, Pan Y, Chen G, Lin W (2012) Extension of the growing season due to delayed autumn over mid and high latitudes in North America during 1982–2006. Global Ecology and Biogeography, **21**, 260-271.

Figure legends

Figure 1. Change of EOS determined by the average of four EOS extraction methods and corresponding climatic variables during the periods from 1982 to 2011. The period of each climatic variable was defined as the period that highest correlation coefficient was determined by the simple linear correlation analysis between each climatic variable and EOS. Dotted regions indicated the detected trends were significant at P <0.05.

Figure 2. Spatial pattern of partial correlation coefficient and simple correlation coefficient between climatic factors and EOS determined by the average of four individual methods. Fig. 2a-c were the results of temperature, precipitation and insolation using partial correlation, while Fig. 2d-f were calculated using simple correlation. Doted regions indicated correlations were significant at $P < 0.05$.

Figure 3. Distribution of the dominant climatic factors of EOS determined by the average of four individual methods (a) and their variation along the gradient of mean annual temperature, precipitation and insolation (b-d). Red (temperature), blue (precipitation) and green (insolation) were applied to indicate which factor was more dominant in each pixel.

Figure 4. Spatial pattern of partial (Fig. 4a) and simple correlation (Fig. 4b) coefficient between EOS and SOS determined by the average of four individual methods. Partial correlation coefficient was calculated after controlling climatic factors (i.e. temperature, precipitation and insolation). Doted regions indicated correlations were significant at $P < 0.05$.

Figure 5. Partial correlations coefficient between EOS, SOS and climatic variables of each biome determined by average of four methods. Bars above 0 represented percentage of

positive correlations, while the remaining showed negative percentages. Colored part indicated percent of significant correlations at $P < 0.05$.

Table 1 Summary of four widely applied methods in determine the date of EOS using satellite based NDVI records.

Methods	Data filter function	Determination of EOS	Reference
Hants-Mr	$NDVI(\mathrm{t}) = a_0 + \sum_{i=1}^{n} a_i \cos(\omega_i t - \varphi_i)$	Maximum decrease in fitted NDVI	(Jakubauskas *et al.*, 2001; De Wit & Su, 2005)
Polyfit-Mr	$NDVI(t) = \alpha_0 + \alpha_1 t^1 + \alpha_2 t^2 + ... + \alpha_6 t^6$	Maximum decrease in fitted NDVI	(Piao *et al.*, 2006)
Double logistic	$NDVI(\mathrm{t}) = \mathrm{wNDVI} + (\mathrm{mNDVI} - \mathrm{wNDVI}) \times \left(\frac{1}{1+e^{-mS(\mathrm{t}-S)}} + \frac{1}{1+e^{mA(\mathrm{t}-\mathrm{A})}} - 1 \right)$ $NDVI(\mathrm{t}) = \mathrm{mNDVI} - (\mathrm{mNDVI} - \mathrm{wNDVI}) \times \left(\frac{1}{1+e^{-mS(\mathrm{t}-\mathrm{S})}} + \frac{1}{1+e^{mA(\mathrm{t}-\mathrm{A})}} - 1 \right)$	model parameter A	(Pinty *et al.*, 2007; Julien & Sobrino, 2009)
Piecewise logistic	$NDVI(t) = \begin{cases} \frac{c_1}{1+e^{a_1+b_1 t}} + d_1 & t \le \alpha \\ \frac{c_2}{1+e^{a_2+b_2 t}} + d_2 & t > \alpha \end{cases}$	Local minima for the derivatives of fitted NDVI curve	(Zhang *et al.*, 2003; Zhang *et al.*, 2007)

Data filter function was used to reconstruct time series NDVI curve from satellite data which could be potentially interrupted by residue noise from cloud contamination and unstable atmosphere conditions. Afterwards, predefined criteria used to determine the date of EOS was applied. In the data filter function, t is Julian date, and NDVI(t) indicates the value of NDVI at Julian day t. The remaining coefficients can be estimated using iterative nonlinear least square technique (i.e. L-M method).

Figure 1

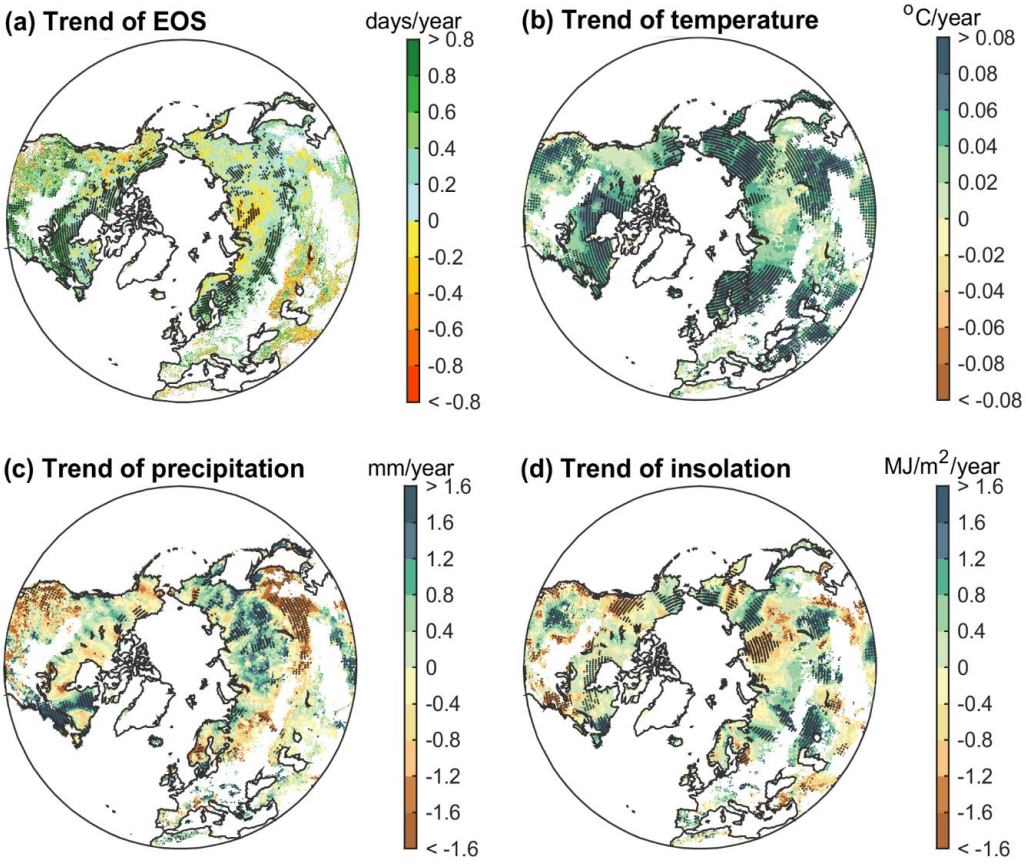
(a) Trend of EOS
days/year
> 0.8
0.8
0.6
0.4
0.2
0
-0.2
-0.4
-0.6
-0.8
< -0.8
(b) Trend of temperature
°C/year
> 0.08
0.08
0.06
0.04
0.02
0
-0.02
-0.04
-0.06
-0.08
< -0.08
(c) Trend of precipitation
mm/year
> 1.6
1.6
1.2
0.8
0.4
0
-0.4
-0.8
-1.2
-1.6
< -1.6
(d) Trend of insolation
MJ/m2/year
> 1.6
1.6
1.2
0.8
0.4
0
-0.4
-0.8
-1.2
-1.6
< -1.6

Figure 2

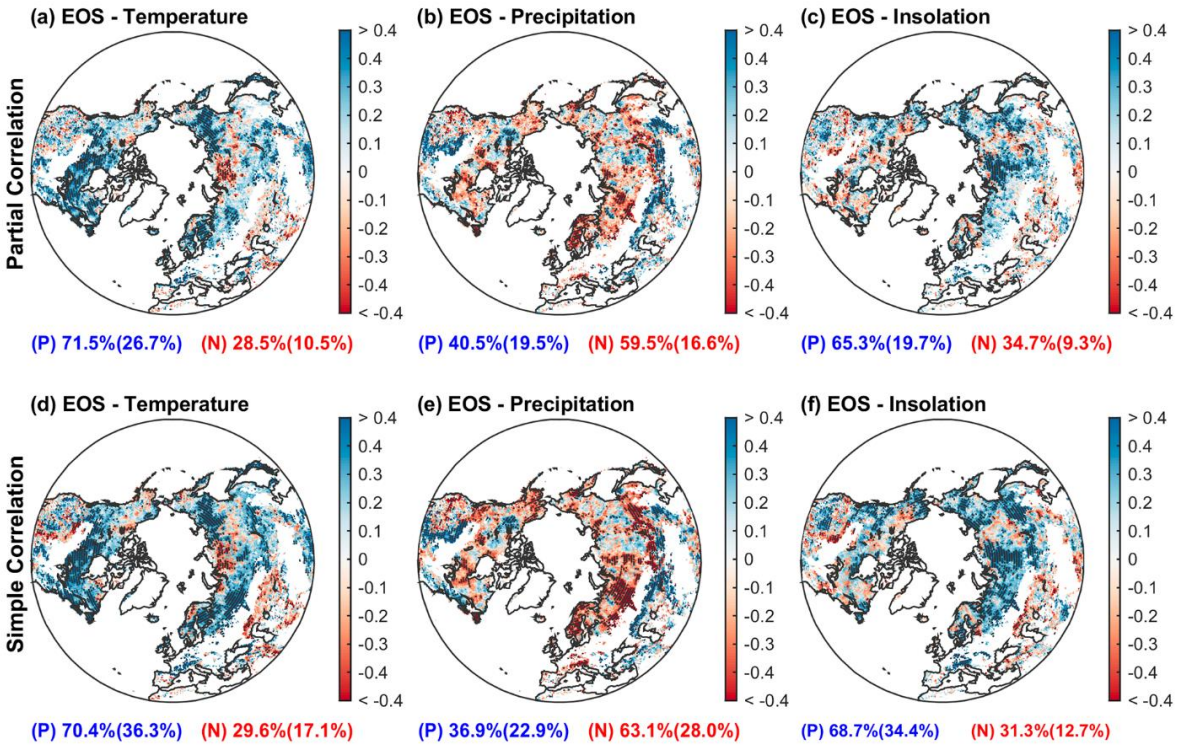
(a) EOS - Temperature
(b) EOS - Precipitation
(c) EOS - Insolation
Partial Correlation
> 0.4
0.4
0.3
0.2
0.1
0
-0.1
-0.2
-0.3
-0.4
< -0.4
(P) 71.5%(26.7%) (N) 28.5%(10.5%)
(P) 40.5%(19.5%) (N) 59.5%(16.6%)
(P) 65.3%(19.7%) (N) 34.7%(9.3%)
(d) EOS - Temperature
(e) EOS - Precipitation
(f) EOS - Insolation
Simple Correlation
(P) 70.4%(36.3%) (N) 29.6%(17.1%)
(P) 36.9%(22.9%) (N) 63.1%(28.0%)
(P) 68.7%(34.4%) (N) 31.3%(12.7%)

Figure 3

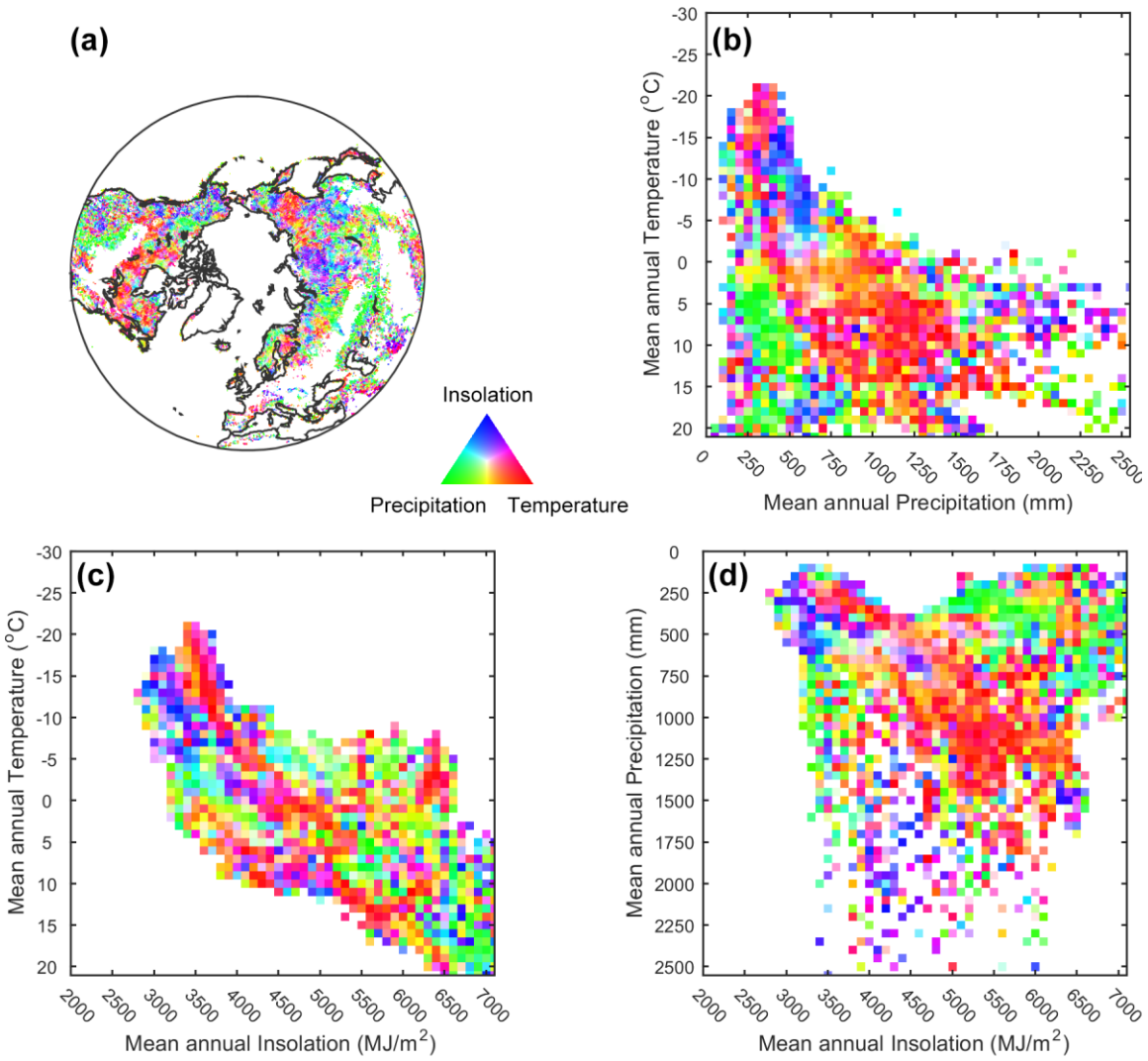
(a)
Insolation
Precipitation
Temperature
(b)
Mean annual Temperature (°C)
Mean annual Precipitation (mm)
(c)
Mean annual Temperature (°C)
Mean annual Insolation (MJ/m2)
(d)
Mean annual Precipitation (mm)
Mean annual Insolation (MJ/m2)

Figure 4

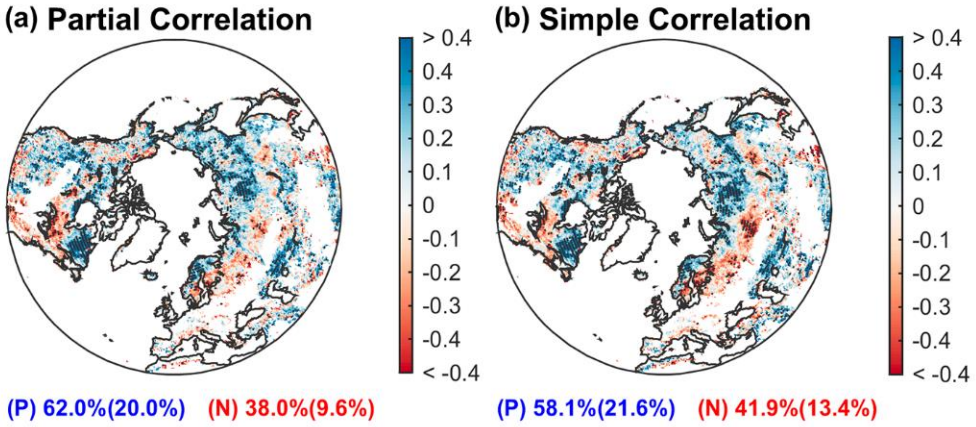
(a) Partial Correlation
> 0.4
0.4
0.3
0.2
0.1
0
-0.1
-0.2
-0.3
-0.4
< -0.4
(P) 62.0%(20.0%)
(N) 38.0%(9.6%)
(b) Simple Correlation
> 0.4
0.4
0.3
0.2
0.1
0
-0.1
-0.2
-0.3
-0.4
< -0.4
(P) 58.1%(21.6%)
(N) 41.9%(13.4%)

Figure 5

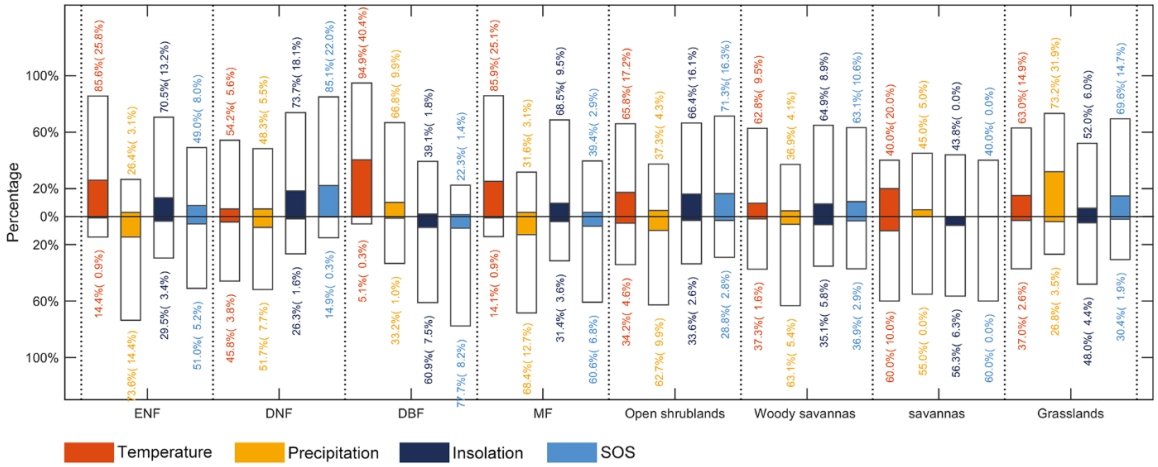
Percentage
100%
60%
20%
0%
20%
60%
100%
ENF
DNF
DBF
MF
Open shrublands
Woody savannas
savannas
Grasslands
Temperature
Precipitation
Insolation
SOS